COMPUTATIONAL MODELLING OF CONCRETE FRACTURE

RENÉ DE BORST[1]
Delft University of Technology, Faculty of Civil Engineering
P.O. Box 5048, NL-2600 GA Delft, The Netherlands

ABSTRACT

Some of the most important aspects of numerical modelling of cracking in concrete are reviewed. After a discussion of the three main lines in modelling cracking - discrete crack models, smeared representations and approaches using lattice models - a concise treatment including comparative studies is given of the various smeared crack approaches that exist to date. Next a discussion is presented of some issues pertaining to the sensitivity of numerical results on the fineness of the mesh and the direction of the mesh lines.

KEYWORDS

Concrete, cracking, finite element method, localisation, non-local continuum

INTRODUCTION

Three main approaches exist for modelling cracking in concrete, mortar, masonry and rocks, namely discrete crack models (Ngo and Scordelis, 1967), smeared-crack models (Rashid, 1968), while recently the lattice models (van Mier *et al.*, 1994) have become popular for explaining fracture processes at a detailed level.

In the first method cracking is assumed to occur as soon as the nodal force that is normal to the element boundaries exceeds the maximum tensile force that can be sustained. New degrees-of-freedom at that node location are created and a geometrical discontinuity is assumed to occur between the 'old' node and the newly created node. In the second route of modelling the cracking process is lumped into the integration points within the elements, where the stress-strain relation is modified to account for the stiffness and strength degradation that accompanies cracking. Finally, in lattice models, originally devised by physicists (Herrmann *et al.*, 1989), the continuum is replaced a priori by lattices of truss or beam elements. Subsequently, the microstructure of the material can be mapped onto these beam elements by assigning them different properties, depending whether the truss or beam element represents a grain or mortar.

Two main improvements with respect to discrete crack models are the possibilities of remeshing and the use of interface elements as predefined cracks. Remeshing techniques were devel-

1. Also at: Eindhoven University of Technology, Faculty of Mechanical Engineering

oped by Ingraffea and Saouma (1985). Using linear-elastic fracture mechanics techniques it is decided where, and in which direction a crack will propagate. Then, a new mesh is formed in which the crack has propagated over a certain distance. Care must be taken that a proper refinement is applied near the crack tip and that special elements are used which can capture the stress singularity at the crack tip in the linear-elastic solution. A new linear-elastic fracture mechanics analysis is carried out for this geometrically changed structure and on the basis of newly determined stress intensity factors a new propagation direction is decided upon. Crack extension is assumed in this new direction and a new mesh is set up. The process can then be repeated until complete failure.

While this procedure basically consists of a series of linear-elastic calculations, albeit in an automatised manner, the approach of Rots (1988) to use interface elements as predefined cracks is essentially a fully non-linear approach. In his procedure interface elements of zero thickness are inserted in the finite element mesh at locations at which a crack is expected to propagate. These locations are chosen either on the basis of smeared-crack analyses or by assessment of experimental data. The interface elements have dual nodes, which have the same coordinates. As in continuum elements the stresses are sampled in integration points between the individual node sets. When the normal stress in an integration remains below the tensile strength the stress-strain relation in the interface is taken as linear elastic, with a high dummy stiffness in order to practically suppress deformations in the interface. When the tensile strength is exceeded in an integration point the unbalanced force thus generated may cause displacements between the two nodes of the node-sets of the interface. We obtain opening (mode-I behaviour) as well as sliding (mode-II behaviour) along the interface element. Of course, the success of this approach crucially depends on a correct estimate of the crack propagation path. Furthermore, the approach is primarily applicable to localised failure where we indeed have one dominant crack that leads to failure. If these conditions are not fulfilled a discrete-crack analysis along these lines may be less successful.

The success of accurate predictions of the direction of crack propagation in smeared-crack finite element representations depends to a large extent on the tangential shear stiffness of the constitutive relation. A large number of constitutive models have been proposed in the past, which lead to different predictions for the incremental shear stiffness. Sometimes these differences are large, sometimes they are hardly discernible, which is related to the similarity of some of the fracture formulations.

A possible way to categorise smeared-crack models is to divide them into models that are based on a total formulation, i.e. there exists an injective relation between the stresses and the total strains, and models that employ a linear relation between stress rate and strain rate via a loading history dependent tangential modulus. Examples of the former category are the elasticity-based fixed crack model, the rotating crack model (Cope *et al.*, 1980), a deformation plasticity theory with a Rankine type yield locus (Feenstra and de Borst, 1995) and elasticity-based damage models, either isotropic (Mazars and Pijaudier-Cabot, 1989), or anisotropic. In the second class of models we have the multidirectional crack model (de Borst and Nauta, 1985; de Borst, 1987; Rots, 1988) and the Rankine plasticity model based on a flow theory of plasticity (Feenstra and de Borst, 1995, 1996). Although major conceptual differences underly the various formulations, remarkable similarities exist especially between plasticity-based models and the familiar rotating crack model when typical non-proportional load paths are simulated. On the other hand the classical fixed crack model gives predictions that significantly differ from most of the other approaches, in the sense that the model usually responds too stiff.

In this contribution we shall focus on the topics that have surfaced in the 1980s and have become major issues since then. Specifically, we shall address the issue of crack models, where the emphasis will be on smeared formulations. Then, a discussion will follow of some approaches to overcome pathological mesh sensitivity.

A CATEGORISATION OF SMEARED-CRACK MODELS

Limiting the discussion to grade-1 materials a total stress-strain relation can be defined as

$$\boldsymbol{\varepsilon} = f(\boldsymbol{\sigma}, \boldsymbol{\eta}, \kappa) , \tag{1}$$

with f a tensor-valued function, $\boldsymbol{\varepsilon}$ a strain tensor and $\boldsymbol{\sigma}$ the stress tensor. Eq. (1) assumes the existence of a single tensor-valued internal variable, $\boldsymbol{\eta}$, and a single scalar valued internal variable, κ, which reflect the loading history of the material. Extension of this formulation to include more internal variables poses no fundamental problem, but is not necessary for our present purpose. Alternatively, a constitutive formulation can be phrased in rate format, such that

$$\dot{\boldsymbol{\varepsilon}} = f(\boldsymbol{\sigma}, \dot{\boldsymbol{\sigma}}, \boldsymbol{\eta}, \kappa) , \tag{2}$$

whereby the dots signify differentiation with respect to a virtual time. A subclass of constitutive models that fits within the framework of eq. (2) are the incrementally-linear models,

$$\dot{\boldsymbol{\varepsilon}} = \mathbf{C}(\boldsymbol{\sigma}, \boldsymbol{\eta}, \kappa)\, \dot{\boldsymbol{\sigma}} , \tag{3}$$

with $\mathbf{C}$ a tangential compliance tensor.

A simple model that falls into category (1) is elasticity: $\boldsymbol{\varepsilon} = f(\boldsymbol{\sigma})$, which for linear elasticity reduces to $\boldsymbol{\varepsilon} = \mathbf{C}^{\mathrm{e}}\boldsymbol{\sigma}$, with $\mathbf{C}^{\mathrm{e}}$ the fourth-order elastic compliance tensor with the Young's modulus E and the Poisson's ratio ν as constants for the isotropic case. History dependence can be incorporated in a simple manner by degrading the elastic compliance via a scalar-valued internal parameter ω:

$$\boldsymbol{\varepsilon} = \frac{\mathbf{C}^{\mathrm{e}}\boldsymbol{\sigma}}{1-\omega} . \tag{4}$$

or with $\mathbf{D}^{\mathrm{e}} = [\mathbf{C}^{\mathrm{e}}]^{-1}$,

$$\boldsymbol{\sigma} = (1-\omega)\mathbf{D}^{\mathrm{e}}\boldsymbol{\varepsilon} \tag{5}$$

In this isotropic elasticity-based damage theory the damage variable ω grows from zero to one (complete loss of integrity). Damage growth is possible if the damage loading function

$$f(\varepsilon_{\mathrm{eq}}, \kappa) = \varepsilon_{\mathrm{eq}} - \kappa \tag{6}$$

vanishes. In eq. (6) $\varepsilon_{\mathrm{eq}}$ is the equivalent strain, which can be a function of the strain invariants, the principal strains as in Mazars and Pijaudier-Cabot (1989):

$$\varepsilon_{\mathrm{eq}} = \sqrt{\sum_{i=1}^{3} (< \varepsilon_i >)^2} , \tag{7}$$

with ε_i the principal strains, and $< \varepsilon_i > = \varepsilon_i$ if $\varepsilon_i > 0$ and $< \varepsilon_i > = 0$ otherwise, or the local energy release rate due to damage

$$\varepsilon_{\mathrm{eq}} = \frac{1}{2}\, \boldsymbol{\varepsilon}^{\mathrm{T}}\mathbf{C}^{\mathrm{e}}\boldsymbol{\varepsilon} . \tag{8}$$

The parameter κ starts at a damage threshold level κ_0 and is updated by the requirement that during damage growth $f=0$. In particular, the damage loading function f and the rate of the history parameter κ have to satisfy the discrete Kuhn-Tucker conditions

$$f \leq 0 \quad , \quad \dot{\kappa} \geq 0 \quad , \quad f\dot{\kappa} = 0 \, . \tag{9}$$

Damage growth occurs according to an evolution law $F(\kappa)$ such that

$$\omega = F(\kappa) \, . \tag{10}$$

Isotropic damage models have been used successfully in predictions of crack propagation in plain and reinforced concrete (Mazars and Pijaudier-Cabot, 1989). The disadvantage of an isotropic damage model is that possible compressive strut action is eliminated. This disadvantage particularly holds for the analysis of reinforced concrete structures.

Directional dependence of damage evolution can be incorporated by degrading the Young's modulus E in the direction of the major principal stress. When, for planar conditions, distinction is made between the global x, y-coordinate system and a local n, s-coordinate system aligned with the principal stress axes one obtains in the local coordinate system the secant tangential stiffness relation

$$\boldsymbol{\sigma}_{ns} = {}^{s}\mathbf{D}_{ns}\boldsymbol{\varepsilon}_{ns} \, , \tag{11}$$

with ${}^{s}\mathbf{D}_{ns}$ defined as

$${}^{s}\mathbf{D}_{ns} = \begin{bmatrix} (1-\omega)E & 0 & 0 \\ 0 & E & 0 \\ 0 & 0 & \beta G \end{bmatrix} , \tag{12}$$

with $\omega = \omega(\varepsilon_{nn})$ and $\beta = \beta(\varepsilon_{nn})$ functions of the normal strain in the local n-direction. The (secant) shear reduction factor β represents the degradation of the elastic stiffness G and is gradually reduced from one to zero. Alternatively, β can be assigned a constant value between zero and one.

Let now ϕ be the angle between the n and x axes and assume that the directions of principal stress and strain coincide throughout the damage process. Then, the standard tranformation rules for second order tensors apply:

$$\boldsymbol{\varepsilon}_{ns} = \mathbf{T}(\phi)\boldsymbol{\varepsilon}_{xy} \tag{13}$$

and

$$\boldsymbol{\sigma}_{ns} = \mathbf{T}(\phi)\boldsymbol{\sigma}_{xy} \, , \tag{14}$$

with $\mathbf{T}$ the standard transformation matrix. Combination of eqs. (11), (13) and (14) yields

$$\boldsymbol{\sigma}_{xy} = \mathbf{T}^{T}(\phi)\,{}^{s}\mathbf{D}_{ns}\mathbf{T}(\phi)\boldsymbol{\varepsilon}_{xy} \, . \tag{15}$$

Eq. (15) incorporates the traditional fixed crack model and the rotating crack model. The only difference is that in the fixed crack model the inclination angle ϕ is fixed when the major principal stress first exceeds the tensile strength ($\phi = \phi_0$), while in the rotating crack concept ϕ changes such that the n-axis continues to coincide with the major principal stress direction. This difference has profound consequences when deriving the tangential stiffness, especially with regard to the shear term. For the fixed crack model differentiation of eq. (15) yields

$$\dot{\boldsymbol{\sigma}}_{xy} = \mathbf{T}^{T}(\phi_0)\mathbf{D}_{ns}\mathbf{T}(\phi_0)\dot{\boldsymbol{\varepsilon}}_{xy} \, , \tag{16}$$

with $\mathbf{D}_{ns}$ the local material tangential stiffness matrix:

$$\mathbf{D}_{ns} = \begin{bmatrix} (1-\omega-\omega'\varepsilon_{nn})E & 0 & 0 \\ 0 & E & 0 \\ \beta'\gamma_{ns}G & 0 & \beta G \end{bmatrix} , \tag{17}$$

where the prime signifies differentiation with respect to ε_{nn}. From eq. (17) we observe that for non-constant β the local material tangential stiffness matrix becomes non-symmetric. On the other hand, the requirement of coaxiality between stress and strain tensors that is imposed in the rotating crack model results in a considerably more complicated expression (Bažant, 1983; Willam *et al.* 1986; Rots, 1988)

$$\dot{\boldsymbol{\sigma}}_{xy} = [\mathbf{T}^{T}(\phi)\mathbf{D}_{ns}(\mathbf{I}-\mathbf{L})\mathbf{T}(\phi) + \alpha\mathbf{T}^{T}(\phi)\mathbf{L}\mathbf{T}(\phi)]\dot{\boldsymbol{\varepsilon}}_{xy} \, , \tag{18}$$

with $\mathbf{I}$ the identity matrix, $\mathbf{L} = \mathrm{diag}[0\,,0\,,-1]$, and $\alpha = (\sigma_{nn}-\sigma_{ss})/[2(\varepsilon_{nn}-\varepsilon_{ss})]$. Comparison of (16) and (18) shows that the *tangential* shear stiffness is now given by α instead of βG. As we shall show in the example to be discussed in the next paragraph α can become negative, leading to a reduction of existing shear stresses and thereby also reducing the existence of locked-in stresses (Rots, 1988).

In all formulations discussed above the strains were recoverable. Upon removal of the load the strains vanish. This is not so for a deformation type plasticity model, which can also be cast in the format (1). In it the total strain is partitioned into an elastic part $\boldsymbol{\varepsilon}^{e}$ and an inelastic part $\boldsymbol{\varepsilon}^{i}$, as follows

$$\boldsymbol{\varepsilon} = \boldsymbol{\varepsilon}^{e} + \boldsymbol{\varepsilon}^{i} \, . \tag{19}$$

The elastic strains are related to the stresses via

$$\boldsymbol{\varepsilon}^{e} = \mathbf{C}^{e}\boldsymbol{\sigma} \, . \tag{20}$$

while the inelastic strains are derivable from a plastic potential f

$$\boldsymbol{\varepsilon}^{i} = \lambda \frac{\partial f}{\partial \boldsymbol{\sigma}} \tag{21}$$

where the plastic multiplier λ and $f = f(\boldsymbol{\sigma}\,,\boldsymbol{\eta}\,,\kappa)$ must satisfy the discrete Kuhn-Tucker conditions $\lambda \geq 0$, $f \leq 0$ and $f\lambda = 0$. Accordingly, f also takes the role of a loading function. Combining eqs. (19)-(21) results in

$$\boldsymbol{\varepsilon} = \mathbf{C}^{e}\boldsymbol{\sigma} + \lambda \frac{\partial f}{\partial \boldsymbol{\sigma}} \, , \tag{22}$$

which, upon elaboration, can be shown to fit the format (1).

We now select the Rankine (major principal stress) criterion as loading function and plastic potential and we introduce the reduced stress tensor $\boldsymbol{\xi} = \boldsymbol{\sigma} - \boldsymbol{\eta}$, with $\boldsymbol{\eta}$ the so-called back stress tensor, which governs the amount of kinematic hardening. In a plane-stress configuration the major principal stress can be expressed in terms of the stress vector with aid of Mohr's circle and one obtains

$$f = \sqrt{\tfrac{1}{2}\boldsymbol{\xi}^{T}\mathbf{P}\boldsymbol{\xi}} + \tfrac{1}{2}\boldsymbol{\pi}^{T}\boldsymbol{\xi} - \bar{\sigma}(\gamma\kappa) \tag{23}$$

with the equivalent stress $\bar{\sigma}$ a function of the internal parameter κ, and γ a factor which sets the ratio between kinematic hardening/softening and isotropic hardening/softening. Pure kinematic hardening is obtained for $\gamma = 0$ and $\gamma = 1$ sets the other limiting case of pure isotropic hardening/softening. The projection matrix $\mathbf{P}$ and the projection vector $\boldsymbol{\pi}$ are given by

$$\mathbf{P} = \begin{bmatrix} \frac{1}{2} & -\frac{1}{2} & 0 \\ -\frac{1}{2} & \frac{1}{2} & 0 \\ 0 & 0 & 2 \end{bmatrix} \tag{24}$$

and

$$\boldsymbol{\pi} = [\,1\,,\,1\,,\,0\,]^{\mathrm{T}} \tag{25}$$

respectively. The equivalent stress $\bar{\sigma}(\gamma\kappa)$ is the current uniaxial tensile strength which starts at the initial tensile strength f_t and is gradually reduced according to some tension-softening model. The internal parameter κ is assumed to be a measure for the internal damage and is supposed to be determined by a work-hardening hypothesis

$$\kappa\bar{\sigma} = \boldsymbol{\xi}^{\mathrm{T}}\boldsymbol{\varepsilon}^{\mathrm{i}} \,. \tag{26}$$

The back stress $\boldsymbol{\eta}$ is given by

$$\boldsymbol{\eta} = \lambda(1-\gamma)E_{\mathrm{ks}}\boldsymbol{\Lambda}\frac{\partial f}{\partial \boldsymbol{\sigma}} \,, \tag{27}$$

with E_{ks} a secant stiffness modulus and $\boldsymbol{\Lambda} = \mathrm{diag}[1\,,\,1\,,\,1/2]$. A rationale for this formulation has been given by Feenstra and de Borst (1995).

Alternatively, the Rankine yield criterion (23) can be used within the framework of a flow theory of plasticity. While the strain decomposition (19) and the relation for the elastic strains (20) remain unaffected, a direct expression for the inelastic strain in the sense of eq. (21) is no longer assumed. Instead, an expression for the inelastic strain *rate* is adopted

$$\dot{\boldsymbol{\varepsilon}}^{\mathrm{i}} = \dot{\lambda}\frac{\partial f}{\partial \boldsymbol{\sigma}} \,, \tag{28}$$

where the plastic flow rate $\dot{\lambda}$ must satisfy the Kuhn-Tucker conditions: $\dot{\lambda} \geq 0$, $f \leq 0$ and $f\dot{\lambda} = 0$. In a similar spirit we now have to define evolution equations for the rate of the internal hardening/softening parameter κ

$$\dot{\kappa}\bar{\sigma} = \boldsymbol{\xi}^{\mathrm{T}}\dot{\boldsymbol{\varepsilon}}^{\mathrm{i}} \,, \tag{29}$$

and the back stress rate

$$\dot{\boldsymbol{\eta}} = \dot{\lambda}(1-\gamma)E_{\mathrm{ks}}\boldsymbol{\Lambda}\frac{\partial f}{\partial \boldsymbol{\sigma}} \,. \tag{30}$$

It is noted that differentiation of eqs. (19)-(20) and combination with eq. (28) results in

$$\dot{\boldsymbol{\varepsilon}} = \mathbf{C}^{\mathrm{e}}\dot{\boldsymbol{\sigma}} + \dot{\lambda}\frac{\partial f}{\partial \boldsymbol{\sigma}} \,, \tag{31}$$

which, upon further elaboration can be shown to fall within the format (3).

The fundamental differences of the formulations discussed so far will be elucidated with an elementary problem proposed by Willam *et al.* (1986), in which a plane-stress element with unit dimensions is loaded in biaxial tension and shear. This causes a continuous rotation of the principal strain axes after cracking, as is typical of crack propagation in smeared crack finite element analysis. The element is subjected to tensile straining in the x-direction accompanied by lateral Poisson contraction in the y-direction to simulate uniaxial loading. Immediately after the tensile strength has been violated, the element is loaded in combined biaxial tension and shear strain, Fig. 1. The ratio between the different strain components is given by $\Delta\varepsilon_{xx} : \Delta\varepsilon_{yy} : \Delta\gamma_{xy} = 0.5 : 0.75 : 1$. The reference set of material parameters is: Young's modulus E = 10,000 MPa, Poisson's ratio ν = 0.2, tensile strength f_t = 1.0 MPa. A linear strain softening diagram with a fracture energy $G_f = 0.15 \times 10^{-3}$ N/mm has been used.

The behaviour of the different formulations for smeared cracking can be studied in detail with this problem. The constitutive behaviour will be compared with respect to the shear stress - shear strain behaviour. The first issue which will be treated is the different behaviour of the models formulated in the total strain concept. The comparison between the isotropic damage model, the rotating crack model and the Rankine deformation plasticity model with isotropic and kinematic hardening should make clear which models are capable of predicting a flexible shear stress - shear strain response. The second issue is the comparison of the rotating crack model and the Rankine plasticity model within an incremental format. Because the response of models with a total formulation is in general more flexible than the response of models with an incremental formulation, we expect that the Rankine plasticity model with an incremental formulation will show a less flexible shear stress - shear strain response, but the comparison should provide insight if this less flexible response is still acceptable.

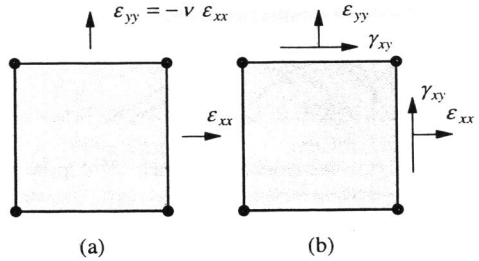

Fig. 1. Tension - shear model problem: (a) tension up to cracking; (b) biaxial tension with shear beyond cracking.

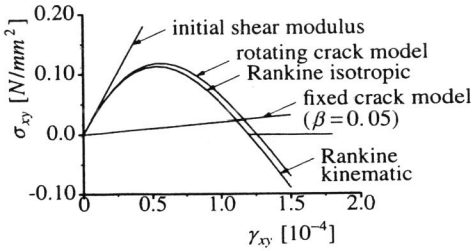

Fig. 2. Total formulation of the constitutive models.

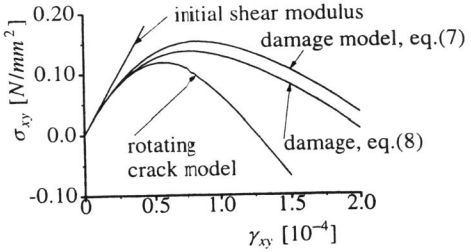

Fig. 3. Damage models and the rotating crack model.

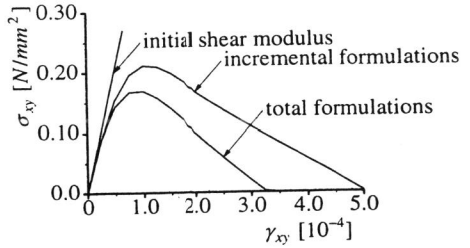

Fig. 4. Elementary tension-shear problem for $G_f = \infty$.

The shear stress - shear strain response of the fixed and rotating crack models and the deformation theory based plasticity models is shown in Fig. 2. The fixed crack model has been used with a shear reduction factor $\beta = 0.05$, which results in a monotonically increasing shear stress with increasing shear strain, Fig. 2. The rotating crack model shows an implicit shear softening behaviour which has been observed previously (Willam *et al.*, 1986; Rots, 1988). It is interesting that the same behaviour occurs for the deformation plasticity model either with isotropic or with kinematic hardening. The two formulations are in fact indiscernible until the shear stress has almost softened completely. Then the isotropic and the kinematic hardening models yield different responses which is due to the fact that with isotropic hardening it is impossible for the shear stress to become negative for positive increments of the shear strain component of the strain vector. It is obvious from Fig. 2 that the differences between the various models are small. Only the fixed crack model gives a completely different response.

Although the tendencies are the same, somewhat larger differences exist between the rotating crack model and the deformation-type plasticity theories on one hand and, on the other hand, the isotropic damage models as formulated in eqs. (5)-(10). In particular the shear stress response is stiffer, although to a lesser extent for the equivalent strain definition via the local energy release rate (eq. (8)) than for that of Mazars (eq. (7)), Fig. 3.

The limiting case with no softening ($G_f = \infty$) confirms that the different formulations within the total strain concept result in a similar behaviour. The shear stress-shear strain responses of the rotating crack model and the Rankine plasticity model are shown in Fig. 4. The response is identical for all models with a total formulation. It is clear from this figure that although no softening has been assumed, the shear stress-shear strain response shows an implicit softening behaviour. Fig. 4 also shows the response of the Rankine model formulated within an incremental concept, which displays a shear stress-shear strain response that is less flexible, but still results in an implicit shear softening.

CRACKING, DAMAGE AND LOCALISATION OF DEFORMATION

A major problem when using a standard, rate-independent continuum for modelling degradation processes such as smeared cracking is that beyond a certain level of damage accumulation the governing set of partial differential equations locally changes type. In the static case the elliptic character of the set of partial differential equations is lost, while, on the other hand, in the dynamic case we observe a change of a hyperbolic set into an elliptic set. In both cases the rate boundary value problem becomes ill-posed and numerical solutions suffer from pathological mesh sensitivity.

The inadequacy of the standard, rate-independent continuum to model failure zones correctly is due to the fact that *force-displacement relations* measured in testing devices are simply mapped onto *stress-strain curves* by dividing the force and the elongation by the original load-carrying area and the original length of the specimen, respectively. This is done without taking into account the changes in the micro-structure that occur when the material is so heavily damaged as in fracture processes. Therefore, the mathematical description ceases to be a meaningful representation of the physical reality.

To solve this problem one must either introduce additional terms in the continuum description which reflect the changes in the micro-structure that occur during fracture, or one must take into account the viscosity of the material. In both cases the effect is that the governing equations do not change type during the damage evolution process and that physically meaningful solutions are obtained for the entire loading range (regularisation procedures). It is emphasised that although concrete can be regarded as a disordered material, the introduction of stochastic distributions of defects does not replace the need for the introduction of regularisation procedures (Carmeliet and de Borst, 1995). For a proper description of failure in concrete both enhancements are necessary: enrichment of the continuum by higher-order terms, either in space or in time, and the introduction of the occurrence of material flaws as a stochastic quantity.

As an intermediate solution between using the standard continuum model and adding higher-order terms the Crack Band Model has been proposed (Bažant and Oh, 1983), in which the area under the softening curve is considered as a material parameter, the so-called fracture energy:

$$G_f = \int \sigma \, \mathrm{d}u = \int \sigma \, \varepsilon(s) \, \mathrm{d}s \, . \tag{32}$$

When we prescribe the fracture energy G_f as an additional material parameter the global load-displacement response can become insensitive to the discretisation. In finite element calculations the crack localises in a band that is one or a few elements wide, depending on the element type, the element size, the element shape and the integration scheme. In Feenstra and de Borst (1996) it is assumed that the width over which the fracture energy is distributed can be related to the area of an element

$$h = \alpha_h \sqrt{A_e} = \alpha_h \left(\sum_{\xi=1}^{n_\xi} \sum_{\eta=1}^{n_\eta} \det(\boldsymbol{J}) \, w_\xi \, w_\eta \right)^{\frac{1}{2}} \tag{33}$$

in which w_ξ and w_η the weight factors of the Gaussian integration rule as it is tacitly assumed

that the elements are integrated numerically. The local, isoparametric coordinates of the integration points are given by ξ and η, and $\det(\boldsymbol{J})$ is the Jacobian of the transformation between the local, isoparametric coordinates and the global coordinate system. The factor α_h is a modification factor which is equal to one for quadratic elements and equal to $\sqrt{2}$ for linear elements (Rots, 1988).

Although the introduction of a fracture energy is a major improvement in calculations using any smeared-crack concept, locally nothing has altered and localisation continues to take place in one row of elements (or better: one row of integration points). This is logical, since the loss of ellipticity still occurs locally, even though the energy that is dissipated remains constant by adapting the softening modulus to the element size. For numerical simulations this implies for instance that severe convergence problems are usually encountered if the mesh is refined or if in addition to matrix failure the possibility of interface debonding between matrix and grains is modelled by inserting interface elements in the numerical model (Rots, 1988). Also, the frequently reported observation still holds that the localisation zones are biased by the discretisation and tend to propagate along the mesh lines.

The deficiency of the standard continuum model with regard to properly describing strain localisation can be overcome by introducing higher-order terms in the continuum description, which are thought to reflect the microstructural changes that take place at a level below the continuum level, for instance crack bridging phenomena in concrete (van Mier, 1991). A number of suggestions have been put forward for non-standard continuum descriptions that are capable of properly incorporating failure zones, see de Borst *et al.* (1993) for an overview. Herein we shall limit ourselves to non-local and gradient damage models.

NON-LOCAL AND GRADIENT DAMAGE MODELS

In a non-local generalisation the equivalent strain ε_{eq} is normally replaced by a spatially averaged quantity (Pijaudier-Cabot and Bažant, 1987):

$$f(\bar{\varepsilon}_{eq}, \kappa) = \bar{\varepsilon}_{eq} - \kappa \ , \tag{34}$$

where the non-local average strain $\bar{\varepsilon}_{eq}$ is computed as:

$$\bar{\varepsilon}_{eq}(\mathbf{x}) = \frac{1}{V_r(\mathbf{x})} \int_V g(\mathbf{s}) \varepsilon_{eq}(\mathbf{x}+\mathbf{s}) \, dV \ , \quad V_r(\mathbf{x}) = \int_V g(\mathbf{s}) \, dV \ , \tag{35}$$

with $g(\mathbf{s})$ a weight function, e.g., the error function, and $\mathbf{s}$ a relative position vector pointing to the infinitesimal volume dV. Alternatively, the locally defined history parameter κ may be replaced in the damage loading function f by a spatially averaged quantity:

$$f(\varepsilon_{eq}, \bar{\kappa}) = \varepsilon_{eq} - \bar{\kappa} \ , \tag{36}$$

where the non-local history parameter $\bar{\kappa}$ follows from:

$$\bar{\kappa}(\mathbf{x}) = \frac{1}{V_r(\mathbf{x})} \int_V g(\mathbf{s}) \kappa(\mathbf{x}+\mathbf{s}) \, dV \ , \quad V_r(\mathbf{x}) = \int_V g(\mathbf{s}) \, dV \ . \tag{37}$$

The Kuhn-Tucker conditions can now be written as:

$$f \le 0 \ , \quad \dot{\kappa} \ge 0 \ , \quad f\dot{\kappa} = 0 \ . \tag{38}$$

Non-local constitutive relations can be considered as a point of departure for constructing gradient models. Again, this can either be done by expanding the kernel ε_{eq} of the integral in (35) in a Taylor series, or by expanding the history parameter κ in (37) in a Taylor series. First, we will expand ε_{eq} and then we will do the same for κ. If we truncate after the second-order terms and carry out the integration implied in (35) under the assumption of isotropy, the following relation ensues:

$$\bar{\varepsilon}_{eq} = \varepsilon_{eq} + \bar{c} \nabla^2 \varepsilon_{eq} \ , \tag{39}$$

where $\bar{c}$ is a material parameter of the dimension length squared. It can be related to the averaging volume and then becomes dependent on the precise form of the weight function g. For instance, for a one-dimensional continuum and taking

$$g(s) = \frac{1}{\sqrt{2\pi} l} e^{-s^2/2l^2} \tag{40}$$

we obtain $\bar{c} = 1/2 \, l^2$. Here, we adopt the phenomenological view that $\sqrt{\bar{c}}$ reflects the length scale of the failure process that we wish to describe macroscopically.

Formulation (39) has a severe disadvantage when applied in a finite element context, namely that it requires computation of second-order gradients of the local equivalent strain ε_{eq}. Since this quantity is a function of the strain tensor, and since the strain tensor involves first-order derivatives of the displacements, third-order derivatives of the displacements have to be computed, which necessitates C^1-continuity of the shape functions. To obviate this problem, eq. (39) is differentiated twice and the result is substituted in eq. (39). Again neglecting fourth-order terms then leads to

$$\bar{\varepsilon}_{eq} - \bar{c} \nabla^2 \bar{\varepsilon}_{eq} = \varepsilon_{eq} \ . \tag{41}$$

When $\bar{\varepsilon}_{eq}$ is discretised independently and use has been made of the divergence theorem, a C^0-interpolation for $\bar{\varepsilon}_{eq}$ suffices (Peerlings *et al.*, 1996).

Higher-order continua require additional boundary conditions. With eq. (41) governing the damage process, either the averaged equivalent strain $\bar{\varepsilon}_{eq}$ itself or its normal derivative must be specified on the boundary S of the body:

$$\bar{\varepsilon}_{eq} = \bar{\varepsilon}_s \quad \text{or} \quad \mathbf{n}^T \nabla \bar{\varepsilon} = \bar{\varepsilon}_{ns} \ , \tag{42}$$

with $\mathbf{n}$ the outward normal vector to the boundary of the body S. In the example calculations the natural boundary condition $\bar{\varepsilon}_{ns} = 0$ has been adopted.

In a fashion similar to the derivation of the gradient damage models based on the averaging of the equivalent strain ε_{eq}, we can elaborate a gradient approximation of (37), i.e., by developing κ into a Taylor series. For an isotropic, infinite medium and truncating after the second term we then have

$$\bar{\kappa} = \kappa + \bar{c} \nabla^2 \kappa \ , \tag{43}$$

where the gradient constant $\bar{c}$ again depends on the weighting function. Interestingly, this expansion directly leads to a formulation in which a C^0-interpolation for κ suffices.

REFERENCES

Bažant, Z.P. (1983). Comment on orthotropic models for concrete and geomaterials. *ASCE J. Eng. Mech.* **109** , 849-865.

Bažant, Z.P. and B. Oh (1983). Crack band theory for fracture of concrete. *RILEM Mat. Struct.* **16** , 155-177.

Borst, R. de (1987). Smeared cracking, plasticity, creep and thermal loading - a unified approach. *Comp. Meth. Appl. Mech. Eng.* **62** , 89-110.

Borst, R. de and P. Nauta (1985). Non-orthogonal cracks in a smeared finite element model. *Engng. Comput.* **2** , 35-46.

Borst, R. de, L.J. Sluys, H.-B. Mühlhaus and J. Pamin (1993). Fundamental issues in finite element analysis of localisation of deformation. *Engng Comput.* **10** , 99-122.

Carmeliet, J. and R. de Borst (1995). Stochastic approaches for damage evolution in standard and non-standard continua. *Int. J. Solids Structures* **32** , 1149-1160.

Cope, R.J., P.V. Rao, L.A. Clark and P. Norris (1980). In: *Numerical Methods for Non-Linear Problems* (C. Taylor, E. Hinton and D.R.J. Owen, eds), Vol. 1, pp. 457-470. Pineridge Press, Swansea.

Feenstra, P.H. and R. de Borst (1995). A plasticity model for mode-I cracking in concrete. *Int. J. Num. Meth. Eng.* **38** , 2509-2529.

Feenstra, P.H. and R. de Borst (1996). A composite plasticity model for concrete. *Int. J. Solids Structures* **33** , 707-730.

Herrmann, H.J. H. Hansen and S. Roux (1989). Fracture of disordered, elastic lattices in two dimensions. *Phys. Rev. B* **39** , 637-648.

Ingraffea, A.R. and V. Saouma (1985). In: *Fracture Mechanics of Concrete,* (G.C. Sih and A. DiTomasso, eds), pp. 171-225. Martinus Nijhoff Publishers, Dordrecht.

Mazars, J. and G. Pijaudier-Cabot (1989). Continuum damage theory - application to concrete. *ASCE J. Eng. Mech.* **115** , 345-365.

Mier, J.G.M. van (1991). Mode-I fracture of concrete: discontinuous crack growth and crack interface grain bridging. *Cement Concrete Res.* **21** , 1-15.

Mier, J.G.M. van, A. Vervuurt and E. Schlangen (1994). In: *Fracture and Damage in Quasibrittle Structures,* (Z.P. Bažant, Z. Bittnar, M. Jirasek and J. Mazars, eds), pp. 289-302. E & FN Spon, London.

Ngo, D. and A.C. Scordelis (1967). Finite element analysis of reinforced concrete beams. *J. Amer. Concrete Institute* **64** , 152-163.

Peerlings, R.H.J., R. de Borst, W.A.M. Brekelmans and J.H.P. de Vree (1996). Gradient-enhanced damage for quasi-brittle materials, *Int. J. Num. Meth. Eng.*, in press.

Pijaudier-Cabot, G. and Z.P. Bažant (1987). Nonlocal damage theory, *ASCE J. Eng. Mech.* **113** , 1512-1533.

Rashid, Y.R. (1968). Analysis of prestressed concrete pressure vessels. *Nucl. Engng. Des.* **7** , 334-344.

Rots, J.G. (1988). *Computational Modeling of Concrete Fracture.* Dissertation, Delft University of Technology, Delft.

Willam, K., E. Pramono and S. Sture (1986). In: *Proc. SEM/RILEM Int. Conf. Fracture of Concrete and Rock* (S.P. Shah and S.E. Swartz, eds), pp. 142-157.